

3-D Image Reconstruction Techniques for Plant and Animal Morphological Analysis - A Review

Anisur Rahman^{1,2}, Changyeun Mo³, Byoung-Kwan Cho^{1*}

¹Department of Biosystems Machinery Engineering, College of Agricultural and Life Science, Chungnam National University, 99 Daehak-ro, Yuseong-gu, Daejeon 34134, Republic of Korea

²Department of Farm Power and Machinery, Bangladesh Agricultural University, Mymensingh 2202, Bangladesh

³National Institute of Agricultural Science, Rural Development Administration, 310 Nonsaengmyeong-ro, Wansan-gu, Jeonju-si, Jeollabuk-do 54875, Republic of Korea

Received: September 26th, 2017; Revised: October 25th, 2017; Accepted: November 27th, 2017

Abstract

Purpose: This review focuses on the major 3-D image reconstruction techniques and their applications in plant and animal morphological analysis. **Methods & Results:** This paper begins with an overview of major 3-D image reconstruction techniques and their basic principles. Subsequently, their applications in plant and animal morphological analysis are reviewed. A discussion on the limitations and future research direction of 3-D imaging techniques for accurate, fast measurements and modeling of plant and animal morphological analysis follows. **Conclusions:** Owing to the increasing demand for plant and animal morphological analysis, the application of 3-D imaging techniques will increase in popularity among researchers and the agricultural industry.

Keywords: 3-D imaging technique, Animal morphology, Plant morphology

Introduction

Precision agriculture has developed over the last 30 years in order to optimize crop and animal husbandry management. This consists of localized crop and animal management using new technologies such as computer vision techniques. Computer vision techniques allow users to obtain information automatically with objective measurements, contrasting with the difficulty and subjectivity of visual or manual acquisition. One-dimensional (1-D) and two-dimensional (2-D) vision systems have been an integral part of successfully implementing computer vision techniques in the precision agriculture field (Vázquez-Arellano et al., 2016). However, imaging information is often obtained in two dimensions and fails to provide some plant and animal characteristics such as

morphology, growth, or early yield estimation. It is believed that computer vision technology is at an inflection point, impelled toward three-dimensional (3-D) approaches owing to technological improvements and lower device prices in the consumer market (Blais et al., 2004; Vázquez-Arellano et al., 2016). Over the last decade, the number of publications related to agricultural 3-D vision systems has been growing fast. Some factors contributing to this trend are the continuous increases in computer processing power, the decrease in electronic prices and sizes, the increase in solid-state illumination efficiency, the unique non-contact and non-destructive properties of computer vision technology, and the need for greater knowledge and care for individual crops and animals (Vázquez-Arellano et al., 2016). Some existing reviews have detailed different techniques for 3-D image acquisition (Blais et al., 2004; Jarvis et al., 1983), including a few reviews of 3-D vision systems in agricultural, industrial, cultural heritage, medicinal, and criminal investigation (McCarthy

*Corresponding author: Byoung-Kwan Cho

Tel: +82-42-821-6715; Fax: +82-42-823-6246

E-mail: chobk@cnu.ac.kr



et al., 2010; Sansoni et al., 2009; Vázquez-Arellano et al., 2016). However, thus far, there has been no comprehensive review providing insights into the achievements and potential of 3-D image reconstruction techniques for plant and animal morphological analysis.

Therefore, this paper aimed to briefly review the major 3-D image reconstruction techniques and present their applications in plant and animal morphological analysis. The paper has structured as follows: firstly, an overview of major 3-D imaging techniques is provided, highlighting their main applications. Secondly, insight into the results achieved in plant and animal morphological analysis is provided; and finally, the limitations and future research directions of 3-D image reconstruction techniques are discussed with regard to accurate, fast measurements and modeling for plant and animal morphological analysis.

Overview of major 3-D imaging techniques

Different techniques are currently used to obtain 3-D image data or depth information of objects. The various 3-D image reconstruction techniques can be broadly classified into active and passive methods (Sansoni et al., 2009; Pankaj et al., 2013). Active methods involve specifically controlling lighting or illumination to obtain 3-D data whereas, in essence, passive methods depend only on ambient light. Active methods are generally less challenging, as illumination can be controlled (Pankaj et al., 2013). However, different techniques have different advantages depending on their application. Some techniques commonly used for plant and animal morphological analysis are described in the section below.

Structure-from-motion technique

Structure-from-motion (SfM) is a range imaging technique that estimates 3-D structuring from a series of 2-D images captured at different points around a scene (Varga and Jadlovský, 2016). These methods are essentially comprised of the following steps: camera calibration and orientation, image point measurements, 3-D point cloud generation, surface generation, and texture mapping (Westoby et al., 2012; Vázquez-Arellano et al., 2016). These techniques differ fundamentally from 2-D imaging techniques, in that the geometry of the scene, camera positions, and orientation are solved automatically without the need to specify a priori (a network of targets with known 3-D positions). Instead, these are solved simultaneously using a highly redundant iterative bundle

adjustment procedure based on a database of features automatically extracted from a set of multiple overlapping images (Sansoni et al., 2009; Chiabrando et al., 2015). This approach is best suited to sets of images with a high degree of overlap capturing the full 3-D structure of the scene viewed from a wide array of positions, or, as the name suggests, images derived from a moving sensor (Chiabrando et al., 2015).

Stereo vision technique

Stereo vision is the best-known passive imaging technique for 3-D image reconstruction (Fig. 2). It requires only a pair of cameras concurrently capturing the same scene (Rovira-Mas et al., 2006). Detecting conjugate pairs in stereo images is a challenging research problem known as the correspondence problem; i.e., for each point in the left image, finding the corresponding point in the right one (Lazaros et al., 2008). The depth is calculated by triangulation based on the disparity of each pixel (difference between the two corresponding points), representing homologous points in the scene (Varga and Jadlovský, 2016). The remarkable advantages of the

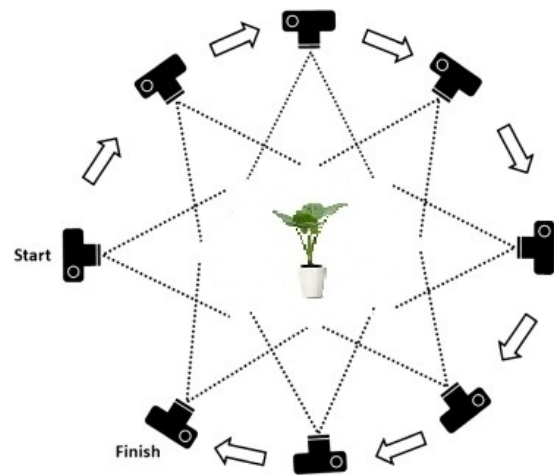


Figure 1. SfM technique adopted from Westoby et al., 2012.

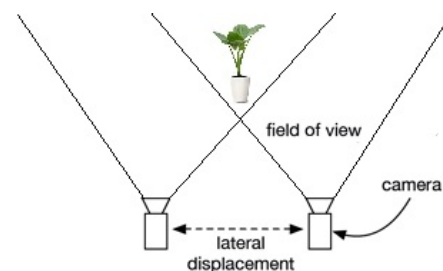


Figure 2. Stereo vision technique.

stereo approach are its simplicity and low cost, because of no further equipment (e.g. specific light sources) nor special projections are required; however, stereo vision also has its drawbacks (Vázquez-Arellano et al., 2016). Stereo vision has significant applications in robotics and computer vision, where problems revolve not around the accurate acquisition of high-quality data, but, rather, around their interpretation (e.g. motion planning, collision avoidance, or grasping applications).

Structured-light technique

The structured-light technique measures the depth of a scene by recording projected light patterns with a camera. A sequence of known patterns is sequentially projected onto an object, which is deformed by the geometry of the object. The object is then observed by a camera from a different direction (Barone et al., 2012; Sarbolandi et al., 2015). By analyzing the distortion of the observed pattern and width of individual stripes, depth information can be extracted. Several patterns (e.g. stripes of varying widths) are typically used per scan (Fig. 3). While this technique has advantageous low hardware costs and high scanning speeds, it requires a controlled environment and projector calibration (Varga and Jadlovský, 2016).

Laser triangulation technique

Laser triangulation systems are also commonly used to acquire depth information from an object. As shown in Figure 4, the laser triangulation system for acquiring 3-D data consists of three main parts: the laser, the detector, and a lens before the detector focusing the beam on the detector (Pankaj et al., 2013). The detector is normally a charged couple detector (CCD) array. In this case, the

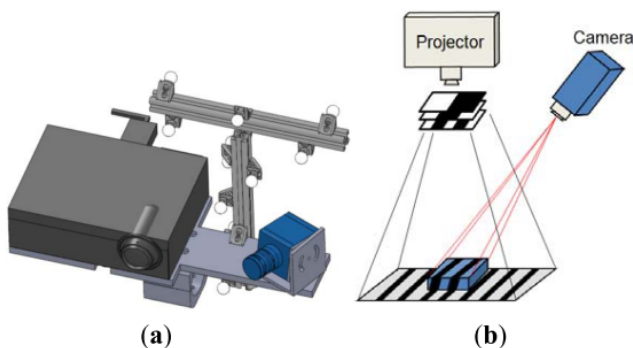


Figure 3. Structured-light technique diagrams (a) with fringe pattern projection (b) adopted from (Barone et al., 2012).

laser diode projects the laser light on the scanned object, which is simultaneously received by the detector through the lens. The detector processes variations in the position of the reflected light related to the shape of the object. Thus, the position of the spotlight on the detector provides range or height information for the object (Pankaj et al., 2013). This technique offers extremely accurate depth measurements and is relative insensitive to illumination conditions or surface texture effects; however, it struggles to correctly scan transparent or reflective surfaces. The results of this technique yield no color or light intensity information.

Time of flight technique

The 3-D surface information of an object can be obtained in real time using the time-of-flight (ToF) principle (shown in Fig. 5). An IR wave, indicated in red, is emitted onto the target object at an intensity modulated by a cosine-shaped frequency signal. The reflected light, indicated in blue, is captured by a sensor and the phase difference between the emitted and reflected lights is used to calculate the depth of the object. The depth is

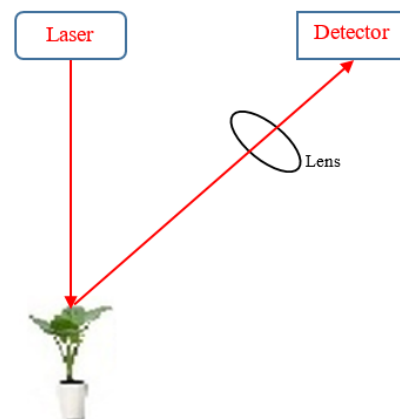


Figure 4. General configuration of a laser triangulation system (Munaro et al., 2015).

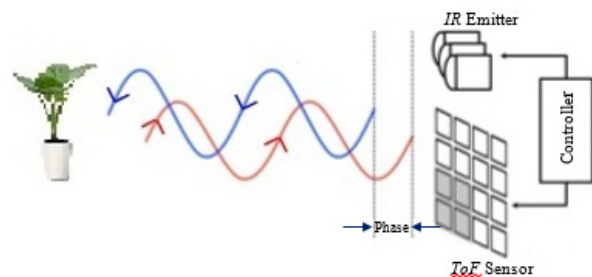


Figure 5. The ToF measurement principle (Hansard et al., 2012).

given by equation (1), where c represents the velocity of light, d the distance traveled by the light, f_{mod} the modulation frequency, and $\Delta\phi$ the phase shift (Hansard et al., 2012).

$$d = \frac{c}{2} \frac{\Delta\phi}{2\pi f_{\text{mod}}} \quad (1)$$

For large measurement ranges, ToF sensors give excellent results. Conversely, for smaller objects (~ 1 m), very high-speed timing circuitry is required. Additionally, ToF sensors have difficulty with shiny surfaces, which reflect little back-scattered light energy except when oriented perpendicularly to the line of sight (Vázquez-Arellano et al., 2016).

Applications

Applications for plant morphological analysis

Some common morphological plant parameters of interest evaluated using 3-D imaging techniques include main-stem height, size, and inclination; petiole length and initiation angle; and leaf width, length, inclination, thickness, area, biomass, and growth status. Until recently, most of these observations and their quantification, known also as plant phenotyping, relied on costly and slow human assessments and measurements. The exponential growth of potential in plant science fields such as genomics and breeding make the application of automated methods in plant phenomics vital.

Stereo vision is a powerful technique for measuring canopy structure and plant growth, height, and shape responses in 3-D for plant morphological sensing. Ivanov et al. (1995) developed a stereo vision technique with a pair of images taken from different viewpoints to reconstruct a 3-D maize canopy model, where different simulation procedures were conducted to analyze the geometrical structure of the 3-D plant canopy, including leaf position and orientation and leaf area distribution. Biskup et al. (2007) designed an area-based, binocular stereo vision system for building 3-D models of the soybean canopy and analyzed leaf angles of inclination during drought stress. Jin and Tang (2009) investigated a new corn plant sensing system using real-time stereo vision, testing the system in both laboratory and field conditions on growth-stage corn plants. Experimental

results indicated that the stereo vision system was capable of detecting both separated and overlapping corn plants with 96.7% accuracy. Lati et al. (2013) developed a plant-oriented 3-D stereovision model based on reconstruction using salient feature points on the plant surface and evaluated the ability of the model to estimate plant growth parameters for sunflower, black nightshade, tomato, corn, and cotton species characterized by different canopy geometries and growth stages in field conditions. Wang et al. (2013) developed a two-camera stereo vision-based system for automated, rapid, and accurate yield estimations of red and green apple orchards, showing a 3.2% estimation error for the red apple block and 1.2% for the green apple block. Xiong et al. (2017) established a high-throughput stereo-imaging system for reconstructing a rape seedling 3-D canopy structure from which leaf areas and plant heights were extracted and compared to manual measurements, showing the mean absolute percentage errors for automatic leaf area and plant height measurements were 3.68 and 6.18%, respectively, whereas the coefficient of determination (R^2) values were 0.984 and 0.845, respectively. Andersen et al. (2005) investigated the potential of using area-based binocular stereo vision for 3-D analysis of single young wheat plants and estimated geometric attributes (e.g. height and total leaf area) for the single wheat plant. Müller-Linow et al. (2015) developed a software package providing tools for quantification of leaf surface properties within natural canopies via 3-D reconstruction from stereo images.

Additionally, the SfM and multi view stereo vision based combined methods are widely used for 3-D reconstruction to phenotype plants. Rose et al. (2015) applied SfM and multi-view stereo techniques to reconstruct a tomato canopy and analyzed single leaf areas, cumulated leaf areas, main stem heights, and convex hull of the complete plant via extraction from 3-D point clouds and comparison with the reference data regarding accuracy and correlation. Lou et al. (2014) described an accurate multi-view stereo alongside SfM 3-D reconstruction method for plants using multi-view images, which accounted for both accuracy and efficiency. Several plants, including *Arabidopsis*, wheat, and maize, were used to evaluate the performance of this reconstruction algorithm. Miller et al. (2015) developed a low-cost hand-held camera alongside SfM with multi-view stereo vision technique to accurately measure the height, crown

depth, crown spread, stem diameter, and volume of small potted trees with R^2 values of 0.982, 0.975, 0.872, 0.935, and 0.951, respectively.

Using the stereo vision technique, some areas of 3-D reconstruction model might not have been covered sufficiently. A SfM technique was proposed to improve surface representations and construct 3-D plant models using automated feature extraction and key point matching across images (Zhang et al., 2016). The SfM technique of simultaneously estimating camera positions and orientations and 3-D scene structures derived from an unordered image dataset (Fonstad et al., 2013). This technique can mitigate the self-occlusion problem in the stereovision method. Zhang et al. (2016) developed a high-efficiency SfM algorithm technique to measure the leaf width/length and stem height/diameter of nursery paprika plants, and evaluated the accuracy of 3-D models reconstructed from photos taken at four different positions. Their results demonstrated that the differences between estimated and measured values were insignificant, and the root-mean-square errors (RMSE) for leaf width/length and stem height/diameter were 0.98 and 0.99, respectively. Jay et al. (2015) proposed a 3-D modeling reconstruction using a SfM based method to characterize sunflowers, savoy cabbages, cauliflowers, and Brussels sprouts under outdoor conditions, and the plant heights and leaf areas in the 3-D model were estimated with R^2 values of 0.99 and 0.94, respectively, relative to the actual values. Hu et al. (2015) developed a method of 3-D reconstruction based on SfM to model eggplant, sweet pepper, and cucumber plants, and extracted phenotypic attributes including leaf blade width, leaf blade length, and blade area. Their results demonstrated high accuracy in 3-D reconstruction, and obtained good agreement between measured and calculated blade areas: blade length and maximum width had an $R^2 > 0.95$ for blade area, $RMSE < 4.5$ mm for blade width, and $RMSE < 5.6$ mm for blade length. Paproki et al. (2012) generated a 3-D reconstruction model of a cotton plant from 64 images using commercially available 3-D reconstruction software and presented a novel mesh-based technique developed for high-throughput 3-D analyses of aerial plant parts. Golbach et al. (2016) presented a computer-vision system for tomato and bell pepper seedling phenotyping to identify and segment plant organs (stems and leaves) from the 3-D plant model based on the shape-from-silhouette method.

The laser scanning method allows for non-destructive generation of 3-D point clouds representing spatial structures directly from a plant for estimating parameters such as leaf area, stem height, stem volume, and biomass. Paulus et al. (2013) introduced an adapted surface feature-based technique for automated pointwise classification of wheat plant organs, leaves, and stems, as well as a separation of wheat ears and stems to extract yield parameters from the 3-D laser. These authors also investigated high-precision laser scanning to directly but non-invasively obtain 3-D data to analyze the organs, leaf, and stem of a single barley as well as the architecture of the whole barley plant (Paulus et al., 2014; Paulus et al., 2014). Wang et al. (2017) developed a low-cost 2-D laser scanner-based mobile terrestrial proximal sensing system for 3-D plant structure phenotyping in indoor environments. Tests validated the proposed solution in terms of specific plant structure variables such as leaf area ($R^2 = 0.92$). Overall, this work has pushed forward the development of LiDAR (Light Detection and Ranging)-based plant phenotyping techniques into the real world application/low-cost stage, suggesting that additional practical applications of LiDAR in plant phenotyping may be discovered in communities such as plant cultivation and precision agriculture.

The ToF technique has emerged as an active sensing tool for 3-D model reconstruction to measure plant morphological properties (Dornbusch et al., 2012). Today, there are many commonly known data acquisition methods for these techniques. Among them, LiDAR is typically used for constructing accurate and detailed 3-D models; however, such systems are usually expensive and complex (Zhang et al., 2016). Saeys et al. (2009) investigated the feasibility of using two types of LiDAR sensors for estimating wheat crop density in front of a combine harvester and obtained good crop densities at various driving speeds and machine vibrations, with R^2 values ranging from 0.65 to 0.93 based on the 3-D field reconstruction from laser scans. Chaivivatrakul et al. (2014) demonstrated an automatic corn plant phenotyping system based on 3-D holographic reconstruction using a ToF camera capable of characterizing plant morphological phenotypes with error rates of 7.92% for the stem major axis, 15.20% for the stem minor axis, 7.45% for the stem height, 21.89% for the leaf area, 10.25% for the leaf length, and 11.09% for the leaf angle. Nakarmi and Tang (2012) developed a system for automatically measuring

Table 1. Summary of 3-D imaging techniques for plant morphological analysis

Variety	Measured parameter	Result	Techniques	Reference
Apple	Yield estimation	Error = 3.2% for red apple and 1.2% for green apple	Stereo-vision	(Wang et al., 2013)
Barley plant	Leaf area, stem height, plant height, and plant width	$R^2 = 0.96, 0.92, 0.97$ and 0.86 respectively	Laser scanner	(Paulus et al., 2014)
Barley plant	Leaf area and stem height	$R^2 = 0.99$ and 0.98 respectively	Laser scanner	(Paulus et al., 2014)
Bell pepper	Leaf size, leaf angle, leaf area, and plant height	$R = 0.70, 0.56, 0.55$ and 0.93	Time-of-flight and stereo vision	(van der Heijden et al., 2012)
Cauliflower	Fruit volume	Error below 0.6%	Kinect sensor	(Andújar et al., 2016)
Corn	Plant sensing	Accuracy= 96.7%	Stereo-vision	(Jin and Tang, 2009)
Corn plants	Stem major axis, stem minor axis, stem height, leaf area, leaf length, and leaf angle	Error rate = 7.92%, 15.20%, 7.45%, 21.89%, 10.25% and 11.09%, respectively	Time-of-flight	(Chaivivatrakul et al., 2014)
Cotton	Stem height, leaf width, and leaf length	$R = 0.88, 0.96,$ and 0.95 respectively.	Structure from motion	(Paprocki et al., 2012)
Eggplant, sweet pepper, and cucumber	Leaf blade width, leaf blade length, and blade area	RMSE < 4.5 mm, < 5.6 mm and $R^2 > 0.95$ respectively	Structure from motion	(Hu et al., 2015)
Linden, field maple, walnut, and red maple	Tree height, crown depth, crown spread, stem diameter, and total tree volume	$R^2 = 0.982, 0.975, 0.872,$ 0.935 and 0.951 respectively	Structure from motion and multi-view stereo	(Miller et al., 2015)
Maize	Plant sensing	Accuracy = 80–90%	LIDAR	(Weiss and Biber, 2011)
Maize	Corn plant spacing	$R^2 = 0.95$	Time-of-flight	(Nakarmi and Tang, 2012)
Oilseed rape	Leaf area and plant height	$R^2 = 0.984$ and $0.845,$ respectively	Stereo-vision	(Xiong et al., 2017)
Paprika	Leaf width/length and stem height/diameter	$R^2 = 0.98$ and 0.99 respectively	Structure from motion	(Zhang et al., 2016)
Philodendron 'con-go'	Leaf maximum height, leaf petiole height, leaf tip height, and leaf surface area	$R^2 = 0.98, 0.98, 0.99$ and 0.92 respectively	Laser scanner	(Wang et al., 2017)
Soybean plants	Leaf inclination during drought	Successfully demonstrated	Stereo-vision	(Biskup et al., 2007)
Sugar beet, wheat	Shape of sugar beet taproots, leaves of sugar beets, and shape of wheat ears	$R^2 = 0.93-0.981$	David laser scanner and Microsoft Kinect device	(Paulus et al., 2014)
Sugar beet	Leaf angle distribution	Normalized root mean square error (NRMSE) = 2.5%	Stereo-vision	(Müller-Linow et al., 2015)
Sunflowers, Savoy cabbages, Cauliflowers, and Brussels sprouts	Plant height and leaf area	$R^2 = 0.99$ and 0.94 respectively	Structure from motion	(Jay et al., 2015)
Sunflower, Black nightshade, Tomato, Corn, and Cotton	Plant height, leaf cover area, and biomass	RMSE = 1~1.7 cm, 10~80 cm ² and 0.15~0.26 g respectively	Stereo-vision	(Lati et al., 2013)
Tomato	Leaf area index	Mean absolute percent error (MAPE) = 4.6%	LIDAR	(Hosoi et al., 2011)

Table 1. Summary of 3-D imaging techniques for plant morphological analysis (Continued)

Variety	Measured parameter	Result	Techniques	Reference
Tomato	Single leaf area, cumulated leaf area, main stem height, and convex hull.	$R^2 = 0.99, 0.99, 0.96$ and 0.99 respectively	Structure from motion and multi-view stereo	(Rose et al., 2015)
Tomato and bell pepper seedlings	Stem length, leaf length, leaf width, and leaf area	$R^2 = 0.75, 0.83, 0.69$ ~ 0.73 and 0.72 ~ 0.78 respectively	Shape-from-silhouette	(Golbach et al., 2016)
Wheat	Plant height and total leaf area	$R^2 = 0.82$ and 0.83 respectively	Stereo-vision	(Andersen et al., 2005)
Wheat	Crop density	$R^2 = 0.80$ ~ 0.96	Time-of-flight (LiDAR)	(Saeys et al., 2009)
Wheat	Total ear weight, total kernel weight, and number of kernels	$R^2 = 0.71, 0.66$ and 0.81 respectively	Laser scanner	(Paulus et al., 2013)
Zucchini leaves	Leaf wilting index	$R^2 = 0.903$	Laser scanner	(Zhao et al., 2012)

the distances between corn plants in early growth-stages using a ToF of a light-based 3-D sensor with an overall mean root RMSE of 0.017 m and mean plant misidentification ratio of 2.2%. Van der Heijden et al. (2012) reconstructed the 3-D canopy of tall bell peppers in a greenhouse using combined stereo vision of high-resolution RGB images with low-resolution range ToF images to estimate the leaf size, leaf angle, leaf area and plant height and obtained a good correlation between models and actual measurements with correlation coefficient values of 0.70, 0.56, 0.55, and 0.93, respectively. Hosoi et al. (2011) produced a precise 3-D image of a tomato canopy using a portable high-resolution scanning LiDAR, and leaf areas were accurately estimated with a mean absolute percent error of 4.6%.

Applications for animal morphological analysis

Animal welfare, health monitoring, growth rate, and physiological variables including shape, size and weight are some examples of the many parameters 3-D sensors can be applied to in animal husbandry. Several 3-D imaging techniques can be used as measurements, and are typically performed in an indoor environment (Vázquez-Arellano et al., 2016). Kawasue et al. (2013) used three Kinect sensors to evaluate the weight and size of cattle as well as their postures and shapes with accuracies of up to 93% relative to manual measurements. In another study, these authors (Kawasue et al., 2017) also investigated the body shape and temperature of black cattle using thermography and a Kinect sensor.

Experimental results showed these results were different from manual measurements because of the error caused by the body hair of the cattle. Kuzuhara et al. (2015) used an Xtion depth sensor to estimate relevant parameters in Holstein cows with accuracies of 74%, 80%, 79%, 62%, and 53% for body condition score, body weight, milk yield, milk fat, and milk protein respectively. Menesatti et al. (2014) developed a low-cost stereo pair system to obtain 3-D positioning of Alpagota sheep for body parameter assessments, to indirectly estimate their live weight, and reported a correlation coefficient of 0.79. Pallottino et al. (2015) used also a stereo-vision technique in combination with an image analysis algorithm for measuring body traits in breeding Lipizzan horses, resulting in a correlation coefficient of 0.998 between manual measurements and stereo vision. Wu et al. (2004) developed a stereo imaging system with six high-resolution cameras and three flash units to capture the 3-D shapes of live pigs (side, rear, and top). Shi et al. (2016) combined a binocular stereo vision system with the LabVIEW development platform to analyze and estimate pig body size and live body weight in indoor farm conditions, which calculated the body length and withers height of the body size with mean errors of 1.88 cm and 0.81 cm, and estimated pig body weights via image processing with an error of 1.759 kg. Ju et al. (2004) investigated the 3-D surface anatomy of live pigs by developing a high resolution stereo imaging system to investigate the relationships between diets, pig shape, pig growth, and meat quality.

Table 2. Summary of 3-D imaging technique for animal morphological analysis

Type of animal	Measured parameter	Result	Techniques	Reference
Black cattle	Body shape and temperature	Accuracy = 93%	Thermography and Kinect sensor	(Kawasue et al., 2017)
Cattle	Shape measurement	Error = 7%	Kinect sensor	(Kawasue et al., 2013)
Cow	Body condition score, body weight, milk yield, milk fat, and milk protein	$R^2 = 0.74, 0.84, 0.62, 0.62$ and 0.53 respectively	ASUS Xtion depth sensor	(Kuzuhara et al., 2015)
Horse	Body traits	$R = 0.998$	Stereovision system	(Pallottino et al., 2015)
Pig	Body Shape	RMS deviation = ± 0.6 mm	Stereo imaging system with six high-resolution cameras	(Wu et al., 2004)
Pig	Body length, withers height, and body weight	Error = 1.88 cm, 0.81 cm and 1.759 kg respectively	Binocular stereo system	(Shi et al., 2016)
Pig	Shape	RMSE < 0.1 mm	Stereo imaging system	(Ju et al., 2004)
Sheep	Body weight and size (withers height, chest depth, and body length)	$R = 0.79$ and Error = 3.54~5.02%	Stereovision system	(Menesatti et al., 2014)

Limitation and future aspects

The performance of different 3-D image reconstruction techniques depends strongly on their application. After examining different approaches to 3-D imaging reconstructions of plants and animals, it is clear that reconstruction remains a challenge requiring technological advances and optimal data acquisition techniques. Equipment costs should be reduced with regards to computational power. The processing speed of images is another main issue during 3-D image reconstruction for plants and animals. It is, additionally, a very complex task to select a sensor for 3-D image reconstruction that are needed to consider the measurement time, budget, and expected quality of measurement. The sensor performance also depends on the dimensions, shape, texture, temperature, and accessibility of an object. Sometimes, 3-D imaging sensors may be affected by missing or low-quality data resulting from the optical geometry of the system, type of projector and/or acquisition optical device, measurement technique, and characteristics of the target objects (Vázquez-Arellano et al., 2016). As such, further studies are required to determine how best to integrate 3-D image reconstruction techniques to simultaneously measure all desired parameters, and how to overcome the challenges of image processing speed and cost-effectiveness for online applications.

Conclusion

This work reviewed most of the methods that have been used to acquire 3-D image reconstructions for plant and animal morphological analysis. A number of examples were also shown, referencing experiments conducted in laboratory and field conditions for plant and animal morphological analyses. Almost all these techniques are suitable for applications such as plant and animal morphological analysis. Some 3-D techniques have not been tested or require additional research before being applied to animal morphological analysis. Given the urgent industry and research requirements for advanced and rapid technological and instrument developments, 3-D imaging reconstruction techniques exhibit considerable potential for becoming the dominant methods of plant and animal morphological analysis.

Acknowledgements

This work was supported by the International Collaborative Research and Development Program funded by the Ministry of Trade, Industry and Energy (MOTIE), Republic of Korea.

References

- Andersen, H. J., L. Reng and K. Kirk. 2005. Geometric plant properties by relaxed stereo vision using simulated annealing. *Computers and Electronics in Agriculture* 49(2):219-232.
- Andújar, D., A. Ribeiro, C. Fernández-Quintanilla and J. Dorado. 2016. Using depth cameras to extract structural parameters to assess the growth state and yield of cauliflower crops. *Computers and Electronics in Agriculture* 122:67-73.
- Barone, S., A. Paoli and A. Razonale. 2012. 3D Reconstruction and Restoration Monitoring of Sculptural Artworks by a Multi-Sensor Framework. *Sensors* 12(12):16785-16801.
- Biskup, B., H. Scharr, U. Schurr and U. Rascher. 2007. A stereo imaging system for measuring structural parameters of plant canopies. *Plant, Cell & Environment* 30(10):1299-1308.
- Blais, F. 2004. Review of 20 years of range sensor development. *Journal of Electronic Imaging* 13(1):231.
- Chaivivatrakul, S., L. Tang, M. N. Dailey and A. D. Nakarmi. 2014. Automatic morphological trait characterization for corn plants via 3D holographic reconstruction. *Computers and Electronics in Agriculture* 109:109-123.
- Chiabrando, F., E. Donadio and F. Rinaudo. 2015. SfM for Orthophoto to Generation: A Winning Approach for Cultural Heritage Knowledge. In *ISPRS - International Archives of the Photogrammetry, Remote Sensing and Spatial Information Sciences, XL-5/W7:91-98*.
- Dornbusch, T., S. Lorrain, D. Kuznetsov, A. Fortier, R. Liechti, I. Xenarios and C. Fankhauser. 2012. Measuring the diurnal pattern of leaf hyponasty and growth in *Arabidopsis* - a novel phenotyping approach using laser scanning. *Functional Plant Biology* 39(11):860.
- Fonstad, M. A., J. T. Dietrich, B. C. Courville, J. L. Jensen and P. E. Carbonneau. 2013. Topographic structure from motion: a new development in photogrammetric measurement. *Earth Surface Processes and Landforms* 38(4):421-430.
- Golbach, F., G. Kootstra, S. Damjanovic, G. Otten and Rick van de Zedde. 2016. Validation of plant part measurements using a 3D reconstruction method suitable for high-throughput seedling phenotyping. *Machine Vision and Applications* 27(5):663-680.
- Hansard, M., S. Lee, O. Choi and R. Horaud. 2012. *Time of Flight Cameras: Principles, Methods and Applications*. SpringerBriefs in Computer Science (Vol. 95). London: Springer.
- Hosoi, F., K. Nakabayashi and K. Omasa. 2011. 3-D Modeling of Tomato Canopies Using a High-Resolution Portable Scanning Lidar for Extracting Structural Information. *Sensors* 11(12):2166-2174.
- Hu, P., Y. Guo, B. Li, J. Zhu and Y. Ma. 2015. Three-dimensional reconstruction and its precision evaluation of plant architecture based on multiple view stereo method. *Transactions of the Chinese Society of Agricultural Engineering*, 31(11):209-214.
- Ivanov, N., P. Boissard, M. Chapron and B. Andrieu. 1995. Computer stereo plotting for 3-D reconstruction of a maize canopy. *Agricultural and Forest Meteorology* 75(1-3):85-102.
- Jarvis, R. A. 1983. A Perspective on Range Finding Techniques for Computer Vision. *IEEE Transactions on Pattern Analysis and Machine Intelligence PAMI-5(2):122-139*.
- Jay, S., G. Rabatel, X. Hadoux, D. Moura and N. Gorretta. 2015. In-field crop row phenotyping from 3D modeling performed using Structure from Motion. *Computers and Electronics in Agriculture* 110:70-77.
- Jin, J. and L. Tang. 2009. Corn plant sensing using real-time stereo vision. *Journal of Field Robotics* 26(6-7):591-608.
- Ju, X., J. Paul Siebert, N. J. B. McFarlane, J. Wu, R. D. Tillett and C. Patrick Schofield. 2004. A stereo imaging system for the metric 3D recovery of porcine surface anatomy. *Sensor Review* 24(3):298-307.
- Kawasue, K., T. Ikeda, T. Tokunaga and H. Harada. 2013. Three-dimensional shape measurement system for black cattle using KINECT sensor. *Journal of Circuits, Systems and Signal Process* 4(7):222-230.
- Kawasue, K., K. D. Win, K. Yoshida and T. Tokunaga. 2017. Black cattle body shape and temperature measurement using thermography and KINECT sensor. *Artificial Life and Robotics* 22(4):1-7.
- Kuzuhara, Y., K. Kawamura, R. Yoshitoshi, T. Tamaki, S. Sugai, M. Ikegami and T. Yasuda. 2015. A preliminarily study for predicting body weight and milk properties in lactating Holstein cows using a three-dimensional camera system. *Computers and Electronics in Agriculture* 111:186-193.
- Lati, R. N., S. Filin and H. Eizenberg. 2013. Plant growth parameter estimation from sparse 3D reconstruction based on highly-textured feature points. *Precision Agriculture* 14(6):586-605.

- Lazaros, N., G. C. Sirakoulis and A. Gasteratos. 2008. Review of Stereo Vision Algorithms: From Software to Hardware. *International Journal of Optomechanics* 2(4):435-462.
- Lou, L., Y. Liu, J. Han and J. H. Doonan. 2014. Accurate Multi-View Stereo 3D Reconstruction for Cost-Effective Plant Phenotyping. In: Campilho A., Kamel M. (eds) *Image Analysis and Recognition. ICIAR 2014. Lecture Notes in Computer Science*, vol 8815. London, Springer.
- McCarthy, C. L., N. H. Hancock and S. R. Raine. 2010. Applied machine vision of plants: a review with implications for field deployment in automated farming operations. *Intelligent Service Robotics* 3(4):209-217.
- Menesatti, P., C. Costa, F. Antonucci, R. Steri, F. Pallottino and G. Catillo. 2014. A low-cost stereovision system to estimate size and weight of live sheep. *Computers and Electronics in Agriculture* 103:33-38.
- Miller, J., J. Morgenroth and C. Gomez. 2015. 3D modelling of individual trees using a handheld camera: Accuracy of height, diameter and volume estimates. *Urban Forestry & Urban Greening* 14(4):932-940.
- Müller-Linow, M., F. P. Espinosa, H. Scharf and U. Rascher. 2015. The leaf angle distribution of natural plant populations: assessing the canopy with a novel software tool. *Plant Methods* 11(1):11.
- Munaro, M., E. W. Y. So, S. Tonello and E. Menegatti. 2015. *Efficient Completeness Inspection Using Real-Time 3D Color Reconstruction with a Dual-Laser Triangulation System*. London, Springer.
- Nakarmi, A. D. and L. Tang. 2012. Automatic inter-plant spacing sensing at early growth stages using a 3D vision sensor. *Computers and Electronics in Agriculture* 82:23-31.
- Pallottino, F., R. Steri, P. Menesatti, F. Antonucci, C. Costa, S. Figorilli and G. Catillo 2015. Comparison between manual and stereovision body traits measurements of Lipizzan horses. *Computers and Electronics in Agriculture* 118:408-413.
- Pankaj, D. S., R. Nidamanuri and P. Prasad. 2013. 3-D Imaging Techniques and Review of Products. In *Proc. of International Conference on Innovations in Computer Science and Engineering*, 1-6.
- Paprocki, A., X. Sirault, S. Berry, R. Furbank and J. Fripp. 2012. A novel mesh processing based technique for 3D plant analysis. *BMC Plant Biology* 12(1):63.
- Paulus, S., J. Behmann, A-K. Mahlein, L. Plümer and H. Kuhlmann. 2014. Low-Cost 3D Systems: Suitable Tools for Plant Phenotyping. *Sensors* 14(2):3001-18.
- Paulus, S., J. Dupuis, A. -K. Mahlein and H. Kuhlmann. 2013. Surface feature based classification of plant organs from 3D laserscanned point clouds for plant phenotyping. *BMC Bioinformatics* 14(1):238.
- Paulus, S., J. Dupuis, S. Riedel and H. Kuhlmann. 2014. Automated Analysis of Barley Organs Using 3D Laser Scanning: An Approach for High Throughput Phenotyping. *Sensors* 14(7):12670-12686.
- Paulus, S., H. Schumann, H. Kuhlmann and J. Léon. 2014. High-precision laser scanning system for capturing 3D plant architecture and analysing growth of cereal plants. *Biosystems Engineering* 121:1-11.
- Rose, J., S. Paulus and H. Kuhlmann. 2015. Accuracy Analysis of a Multi-View Stereo Approach for Phenotyping of Tomato Plants at the Organ Level. *Sensors* 15(5):9651-9665.
- Rovira-Mas, F., Q. Zhang, M. Kise and J. F. Reid. 2006. Agricultural 3D Maps with Stereovision. In *2006 IEEE/ION Position, Location and Navigation Symposium*, IEEE 1045-1053.
- Saeyns, W., B. Lenaerts, G. Craessaerts and J. De Baerde-maeker. 2009. Estimation of the crop density of small grains using LiDAR sensors. *Biosystems Engineering* 102(1):22-30.
- Sansoni, G., M. Trebeschi and F. Docchio. 2009. State-of-The-Art and Applications of 3D Imaging Sensors in Industry, Cultural Heritage, Medicine and Criminal Investigation. *Sensors* 9(1):568-601.
- Sarbolandi, H., D. Lefloch and A. Kolb. 2015. Kinect range sensing: Structured-light versus Time-of-Flight Kinect. *Computer Vision and Image Understanding* 139:1-20.
- Shi, C., G. Teng and Z. Li. 2016. An approach of pig weight estimation using binocular stereo system based on LabVIEW. *Computers and Electronics in Agriculture* 129:37-43.
- van der Heijden, G., Y. Song, G. Horgan, G. Polder, A. Dieleman, M. Bink and C. Glasbey. 2012. SPICY: towards automated phenotyping of large pepper plants in the greenhouse. *Functional Plant Biology* 39(11):870.
- Varga, M. and J. Jadlovský. 2016. 3D imaging and image processing-literature review. In *16 Scientific Conference of Young Researchers*, Herľany, Slovakia: Faculty of Electrical Engineering and Informatics Technical University of Kosice, 12-15.

- Vázquez-Arellano, M., H. W. Griepentrog, D. Reiser and D. S. Paraforos. 2016. 3-D Imaging Systems for Agricultural Applications-A Review. *Sensors* 16(5).
- Wang, H., Y. Lin, Z. Wang, Y. Yao, Y. Zhang and L. Wu. 2017. Validation of a low-cost 2D laser scanner in development of a more-affordable mobile terrestrial proximal sensing system for 3D plant structure phenotyping in indoor environment. *Computers and Electronics in Agriculture* 140:180-189.
- Wang, Q., S. Nuske, M. Bergerman and S. Singh. 2013. Automated Crop Yield Estimation for Apple Orchards. In *Experimental Robotics*, Springer, Heidelberg, 745-758.
- Weiss, U. and P. Biber. 2011. Plant detection and mapping for agricultural robots using a 3D LIDAR sensor. *Robotics and Autonomous Systems* 59(5):265-273.
- Westoby, M. J., J. Brasington, N. F. Glasser, M. J. Hambrey and J. M. Reynolds. 2012. "Structure-from-Motion" photogrammetry: A low-cost, effective tool for geoscience applications. *Geomorphology* 179:300-314.
- Wu, J., R. Tillett, N. McFarlane, X. Ju, J. P. Siebert and P. Schofield. 2004. Extracting the three-dimensional shape of live pigs using stereo photogrammetry. *Computers and Electronics in Agriculture* 44(3):203-222.
- Xiong, X., L. Yu, W. Yang, M. Liu, N. Jiang, D. Wu and Q. Liu. 2017. A high-throughput stereo-imaging system for quantifying rape leaf traits during the seedling stage. *Plant Methods* 13(1):7.
- Zhang, Y., P. Teng, Y. Shimizu, F. Hosoi and K. Omasa. 2016. Estimating 3D Leaf and Stem Shape of Nursery Paprika Plants by a Novel Multi-Camera Photography System. *Sensors* 16(6):874.
- Zhao, Y.-D., Y.-r. Sun, X. Cai, H. Liu and P. S. Lammers. 2012. Identify Plant Drought Stress by 3D-Based Image. *Journal of Integrative Agriculture* 11(7):1207-1211.